# Annual Report 2017

## Nansen International Environmental and Remote Sensing Centre

*St. Petersburg, Russia*

*Non-profit international centre for environmental and climate research*
*Founded in 1992*

25 years in science 1992-2017

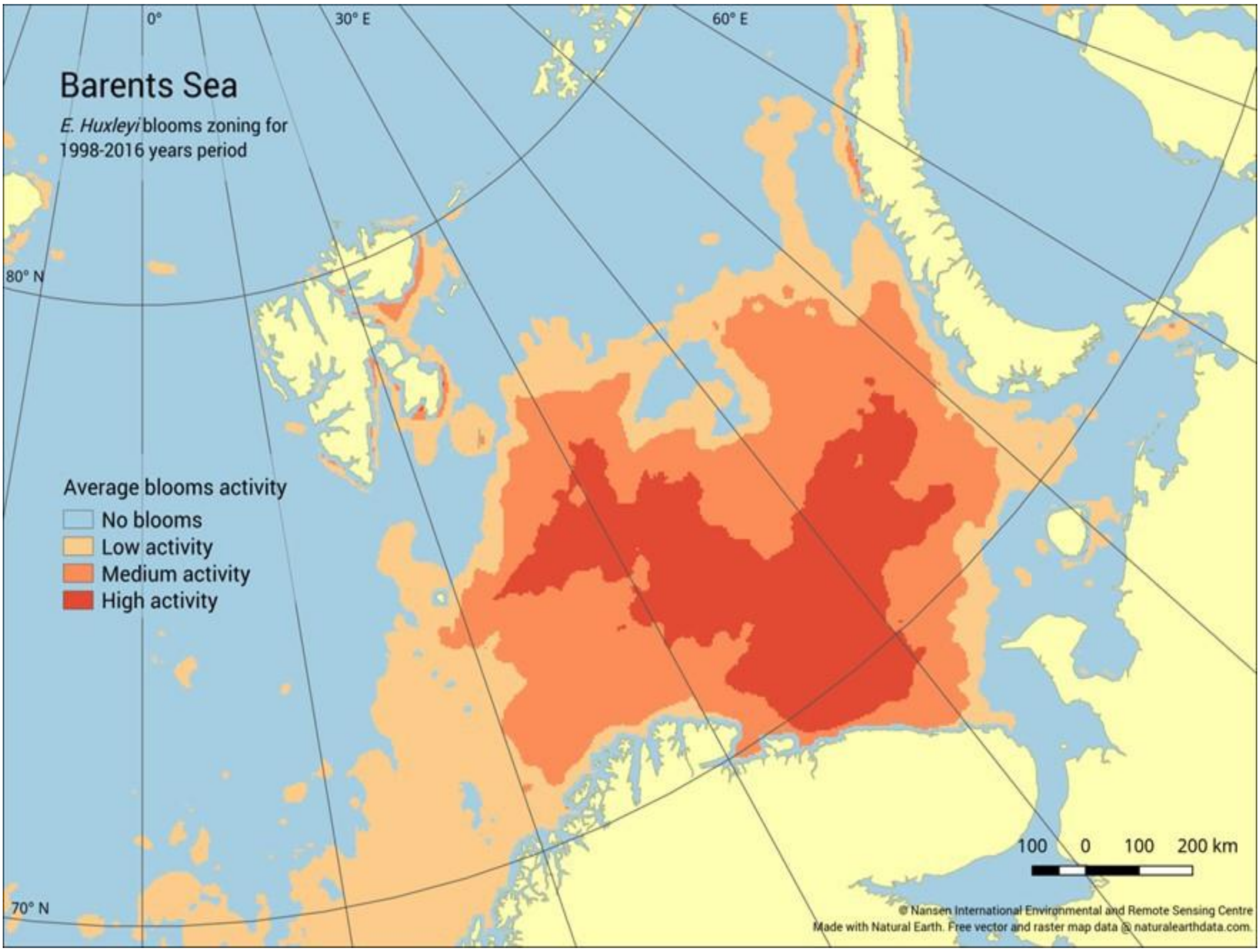

## Founders of the Nansen Centre

**Bergen University Research Foundation (UNIFOB)**
*Bergen, Norway*

**Max-Planck Society (MPS)**
*Munich, Germany*

**Nansen Environmental and Remote Sensing Centre (NERSC)**
*Bergen, Norway*

**Northern Water Problems Institute of Russian Academy of Sciences (NWPI RAS)**
*Petrozavodsk, Republic of Karelia, Russia*

**Saint-Petersburg State University (SPbSU)**
*Saint-Petersburg, Russia*

**Scientific Research Centre for Ecological Safety of RAS (SRCES RAS)**
*Saint-Petersburg, Russia*

With the initial support from
**The Joint Research Centre of the European Commission (JRC EC)**

## Associate Partners of the Nansen Centre

**DLR Maritime Security Lab (DLR MSL)**
*Bremen, Germany*

**Finnish Meteorological Institute (FMI)**
*Helsinki, Finland*

**Global Climate Forum (GCF)**
*Berlin, Germany*

**Helsinki University (HU)**
*Helsinki, Finland*

**Nansen Scientific Society (NSS)**
*Bergen, Norway*

**Stockholm University (SU)**
*Stockholm, Sweden*

## Director

***Dr. Leonid P. Bobylev***

## President

***Prof. Nikolay N. Filatov***
Corresponding Member of Russian Academy of Sciences (RAS); Northern Water Problems Institute of RAS (NWPI RAS)
*Petrozavodsk, Karelia, Russia*

## Co-President

***Prof. Valentin P. Meleshko***
Main Scientist, Voeikov Main Geophysical Observatory (VMGO)
*St. Petersburg, Russia*

## Vice-Presidents

***Prof. Hartmut Grassl***
Max Planck Institute for Meteorology and University of Hamburg (MPIM and UH)
*Hamburg, Germany*

***Prof. Stein Sandven***
Project Leader, Nansen Environmental and Remote Sensing Centre (NERSC)
*Bergen, Norway*

## Board of Guardians

### Chairman

***Prof. Ola M. Johannessen***
President of Nansen Scientific Society (NSS); Founding President of NIERSC; Founding Director of NERSC; Professor Emeritus at the Geophysical Institute, University of Bergen
*Bergen, Norway*

### Members

***Prof. Sergey V. Aplonov***
Vice-Rector, St. Petersburg State University (SPbSU), *St. Petersburg, Russia*

***Prof. Arthur N. Chilingarov***
Corresponding Member, RAS; Special presidential representative for international cooperation in the Arctic and Antarctic, *Moscow, Russia*

***Prof. Ivan Ye. Frolov***
Scientific Supervisor, Arctic and Antarctic Research Institute (AARI), *St. Petersburg, Russia*

***Prof. Matti Leppäranta***
University of Helsinki (UH), *Helsinki, Finland*

***Prof. Valery L. Mikheev***
Rector, Russian State Hydrometeorological University (RSHU), *St. Petersburg, Russia*

***Prof. Igor Mokhov***
Academician, RAS; Director, Institute of Atmospheric Physics of RAS (IAP RAS)
*Moscow, Russia*

***Prof. Timo Vihma***
Head of Polar Meteorology and Climatology Group, Finnish Meteorological Institute (FMI), *Helsinki, Finland*

# REPORT FROM THE GENERAL MEETING OF FOUNDERS

## Vision

The Scientific Foundation "Nansen International Environmental and Remote Sensing Centre" (Nansen Centre, NIERSC) vision is to understand, monitor and predict climate and environmental changes in the high northern latitudes for serving the Society.

## Major Research Areas

Climate Variability and Change in High Northern Latitudes

Aquatic Ecosystems in Response to Global Change

Applied Meteorological and Oceanographic Research for Industrial Activities

Socioeconomic Impact of Climate Change

## Organization

NIERSC is an independent non-profit international research foundation established by Russian, Norwegian and German research organizations. NIERSC conducts basic and applied environmental and climate research funded by the national and international governmental agencies, research councils, space agencies and industry. Additionally, NIERSC receives basic funding from its Founder – Nansen Environmental and Remote Sensing Centre.

NIERSC has been established in 1992 and re-registered in the St. Petersburg Administration Registration Chamber into a non-profit scientific foundation in 2001. The Centre got accreditation at the Ministry of Industry, Science and Technology of the Russian Federation as a scientific institution in 2002 and has been re-registered in 2006 according to a new legislation on Non-Commercial Organizations of the Russian Federation.

NIERSC got a license for conducting meteorological and oceanographic observations from Roshydromet in 2006. In 2008 NIERSC received also a license from Roscosmos for conducting the space-related research activities.

## Staff

At the end of 2017 NIERSC staff incorporated 29 employees comprising core scientists, including one full Doctor of Science and eight PhDs, part-time researchers, and administrative personnel. Six Nansen Fellowship PhD-students were supervised and supported financially, all holding also part-time positions of Junior Scientists at NIERSC.

## Production

In 2017, totally 49 publications have been published, one

***Cover page:** Zoning map of coccolithophores activity in the Barents Sea over 1998-2016.*

book, 13 papers in peer reviewed journals, 6 papers in other journals and 29 conference proceedings (see the list at the end of the report).

## National and International Cooperation

NIERSC has a long-lasting cooperation with Russian organisations such as St. Petersburg State University, institutions of the Russian Academy of Sciences, Federal Space Agency, Federal Service for Hydrometeorology and Environmental Monitoring including the Northern Water Problems Institute, Scientific Research Centre for Ecological Safety, Arctic and Antarctic Research Institute, Russian State Hydrometeorological University, Voeikov Main Geophysical Observatory, Murmansk Marine Biological Institute, Research Centre of Operational Earth Monitoring and other, totally about 40 institutions.

Fruitful relations are established also with number of foreign and international organizations, universities and institutions including European Space Agency, Global Climate Forum, Max-Planck Institute for Meteorology (Germany), Friedrich-Schiller-University (Germany), Finnish Meteorological Institute (Finland), University of Helsinki (Finland), University of Sheffield (UK), Stockholm University (Sweden), Johanneum Research (Austria), and especially with the NIERSC founders. Close cooperation is established with the Nansen Centre in Bergen. Most of scientific results described below are achieved within the joint research activities of both Nansen Centres, in St. Petersburg and Bergen, and cooperating partners.

## Nansen Fellowship Programme

The main objective of the Nansen Fellowship Program (NFP) at NIERSC is to support PhD-students at Russian educational and research institutions, including Russian State Hydrometeorological University, St. Petersburg State University, Arctic and Antarctic Research Institute, and others. The research areas are climate and environmental change and satellite remote sensing, including integrated use of satellite Earth observation techniques in combination with supporting *in situ* observations and numerical modelling for studies of the Earth System. NFP provides PhD-students with Russian and international scientific supervision, financial fellowship, efficient working conditions at NIERSC, training and research visits to foreign research institutions within the Nansen Group and beyond, involvement into international research projects. NFP is sponsored by the Nansen Scientific Society and Nansen Centre in Bergen, Norway. Postgraduate student activity is supervised by at least one Russian and one international senior scientist. All NFP PhD-students obliged to publish their scientific results in the international refereed journals and make presentations at the international scientific symposia and conferences.

Natalia Gnatiuk, the participant of the Nansen Fellowship Programme, has successfully defended her Thesis "Projections of air temperature and precipitation in Ukraine in the 21st century" on 14 April 2017 at the Ukrainian Hydrometeorological Institute, Kiev, Ukraine.

Another participant of the Nansen Fellowship Programme, Valeria Selyuzhenok, has also successfully defended her Thesis "Laptev Sea and East Siberian Sea landfast ice: Mechanism of formation and variability of extent" on 13 October 2017 at the Jacobs University Bremen, Bremen, Germany.

Totally, 28 young Russian PhD-students have got their doctoral degrees with support of NFP since 1994.

## Research Projects

Below is the list of the research projects implemented at NIERSC in 2017 in close cooperation with other national and foreign scientific institutions:

Ships and Waves Reaching Polar Regions (SWARP, EU-FP7, 2014-2017)

Sea Ice CCI (ESA Climate Change Initiative), Phase 2 (ESA/subcontract to NERSC, 2015-2017)

Great Lakes (Michigan Technical University, US, 2016-2017)

Meridional heat and moisture transport into Arctic and its role in the Arctic amplification (Russian Fund for Basic Research (RFBR), 2015-2017)

Development of sea ice monitoring and forecasting system to support safe operations and navigation in Arctic seas (SONARC, Russian-Norwegian Project: RFBR-NORRUS, 2015-2017)

Terrestrial ecosystems and soil carbon accumulation (RFBR, 2015- 2017)

Consumer choice and herding behaviour in microeconomics (RFBR, 2015-2017)

MON-SWARP (Subsidy from Ministry of Education and Science of RF No.14.618.21.0005 for the project "Ships and Waves Reaching Polar Regions", 2015-2017)

Role of soil temperature and moisture in linking the autumn Arctic sea ice and the summer climate over Eurasia (Russian-Chinese Project, RFBR, 2016-2017)

Sea of Okhotsk (Contract to FRECOM, 2017-2018)

Kara Sea (Contract to FRECOM, 2017-2018)

Ladoga-Onega Lakes (s/c to Northern Water Problems Institute, Petrozavodsk, Russia, 2017)

Dynamics of deep oceanic convection in subpolar and polar oceanic regions under the climate change, its relation on freshwater and heat contents and effect on the Atlantic Meridional Overturning Circulation (Russian Science Foundation (RSF), 2017-2019)

Assessment of calcifying phytoplankton role in $CO_2$ dynamics in the atmosphere-ocean system at subpolar and polar latitudes (RSF, 2017-2019)

Complex assessment of polar low impact on maritime activities in the Arctic Ocean under the ongoing climate changes (RSF, 2017-2019)

SAR-based sea ice monitoring in the Arctic (Contract to IANS, 2017-2018)

St. Petersburg, 17 April 2018

*Nikolay N. Filatov, NWPI RAS, President*

*Valentin Meleshko, VMGO, Co-President*

*Hartmut Grassl, Max-Plank Society, Vice President*

*Stein Sandven, NERSC, Vice President*

*Sergey V. Aplonov, SPbSU*

*Andrey A. Tronin, SRCES RAS*

*Leonid P. Bobylev, Director*

# 25TH ANNIVERSARY OF THE NANSEN CENTRE

On 19 October 2017, 25 years have passed since the Nansen International Environmental and Remote Sensing Centre has been established in St. Petersburg. To celebrate this remarkable event, a two-day jubilee scientific symposium has been held on 12-13 October 2017 at Petrovsky Hall of the St. Petersburg State University (first day) and the Nansen Centre premises (second day).

About 100 guests participated in the Nansen Centre's Jubilee Symposium. Among them invited speakers, representatives of the Norwegian Embassy in Moscow and General Consulate in St. Petersburg, NIERSC Founders and Associate Partners, Russian and foreign research institutes and centres including "sister" Nansen Centres in China and India, NIERSC Staff.


*Official opening of the Nansen Centre's 25-year Anniversary Symposium at the Petrovsky Hall of the St. Petersburg State University, 12 October 2017.*

*Top: Symposium Presidium (from the right to the left: Prof. Sergey Aplonov, Vice-Rector, St. Petersburg State University; Prof. Nikolay Filatov, President, Nansen Centre; Mr. Dag Malmer Halvorsen, Consul General of Norway in St. Petersburg; Dr. Leonid Bobylev, Director, Nansen Centre).*

*Right: Symposium participants at the Petrovsky Hall, St. Petersburg State University*

The President of the Nansen Centre, Corresponding Member of the Russian Academy of Sciences, Prof. Nikolay Filatov opened the symposium. Welcome speeches have been delivered by Mr. Dag Malmer Halvorsen, Consul General of Norway in St. Petersburg, and Prof. Sergey Aplonov, Vice-Rector of St. Petersburg State University.

*The second day of symposium at the Nansen Centre premises.*

Symposium programme (see Annex) included invited talks of leading experts in the Earth and Arctic climate systems, global climate change, meteorology, oceanography and satellite observations, and presentations by the NIERSC staff members illustrating past and current research activities at the Nansen Centre.

*Acknowledgement: NIERSC is grateful to the Nansen Scientific Society, Bergen, Norway, for financial support of holding the symposium.*

# Scientific Report

## Climate Variability and Change in High Northern Latitudes

### *Pattern of mean vertical velocity of the Lofoten vortex (Norwegian Sea)*

*Igor Bashmachnikov, Tatyana Belonenko, Pavel Kuibin, Denis Volkov, Victor Foux*

In this work, we focus on a relatively unexplored spatial pattern of the vertical velocity in a subsurface vortex using, as an example, the quasi-permanent anticyclonic Lofoten vortex (LV) in the Lofoten depression of the Norwegian Sea. Formed by relatively weak non-geostrophic velocities in ocean vortices and masked by more intense processes of vortex dynamic instability, mean structure of the circulation in r-z plain in ocean vortices is typically difficult to derive using comparatively short observational time-series. The vertical velocity patterns were obtained for a specific case of the seamounts-trapped quasi-stationary vortices, but these are practically unknown for other types of the open ocean vortices.

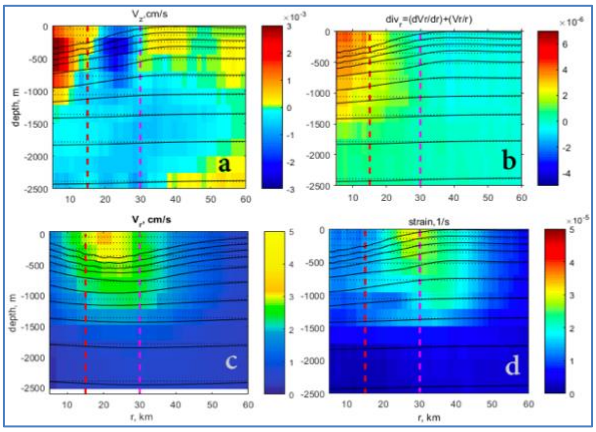


***Figure 1.*** *Radial distribution of time-mean characteristics in LV according to MIT results averaged over 2 years of the model run: **(a)** vertical velocity (positive - upward); **(b)** divergence with radial velocity (positive – directed outwards, $s^{-1}$); **(c)** radial velocity (positive - outwards); **(d)** horizontal shear stresses. Radial distributions of azimuthal velocity (black solid lines) and radial velocity (gray dashed lines) for different vertical levels (out of scale) are offset vertically, referenced to the corresponding horizontal zero-velocity lines at the selected depth levels (dashed). Red and magenta vertical dashed lines mark distances from centre of vortex where depth-mean vertical velocity crosses 0 (12 km) and depth-mean relative vorticity anomaly of LV core crosses 0 (30 km), respectively.*

The anticyclonic LV presents a rare case of an anticyclonic eddy permanently observed over the practically flat central areas of the Lofoten Basin of 3000 m deep. Existing in a relatively calm oceanic background conditions and not rigidly attached to a distinct bottom topography feature, this vortex presents a "natural laboratory" for study of the dynamics of freely propagating mesoscale ocean vortices.

To study LV, we took advantage of the 12-year-long regional simulations of MIT ocean general circulation model. The high-resolution version of this model, used in this study, also provides a realistic horizontal and vertical structure of LV and adequately reproduces the main mechanisms responsible for the permanence of the vortex in the basin.

Evident in *in situ* and MIT results, vertical profiles of temperature and salinity through LV core show positive temperature-salinity anomalies in LV core at mid-depth and negative anomalies over LV core. The colder sea-surface temperature is often observed over subsurface anticyclonic eddies, opposite to what is observed in the sea-surface intensified anticyclones.

Fig. 1 shows time-mean r-z distributions of dynamic characteristics of LV averaged over the period of MIT simulations. The distribution of the vertical velocity has a complex structure indicating a divergence in the upper and lower parts of the vortex. The rise of the water in the central part of the LV above 1300 m (the vortex core and above) is compensated by the water descend at 12-30 km from the vortex axes. This explains the negative upper ocean temperature anomalies over LV discussed above. Water descend integrated over the vortex volume, is about 20% stronger than the integrated water uplift in the vortex centre. It forms the source of mass for the slower water descend below the LV core, near the ocean bottom (Fig. 1a).

The drivers for the observed water divergence are suggested to be the horizontal turbulent diffusion of momentum in the upper and mid-ocean and the Ekman pumping in the bottom boundary layer. Maximum radial divergence is observed in the upper part of the vortex core (Fig. 1b). It is formed by the radial velocities (Fig. 1c), which reach their maximum at 20-25 km from the vortex axis, at the inner boundary of the region of maximum shear stress (25-20 km from the vortex axis), which is also the region of the maximum azimuthal velocities (Fig. 1d). It is expected that the processes of the turbulent diffusion of momentum across the vortex boundary is the most intensive in this region, which drive the observed divergence. The intensity of the Ekman divergence in the bottom boundary layer in the presence of the observed anticyclonic rotation below the LV core is estimated to be sufficient to maintain the resisted downwards motions below 1500 m depth (Fig. 1a).

<u>Relevant publication:</u> *Bashmachnikov, I., Belonenko, T., Kuibin, P., Volkov, D., & Foux, V. Patterns of vertical velocity of the Lofoten vortex (the Norwegian Sea), Ocean Dynamics, submitted.*

### *Pattern distribution of surface waves generated by polar lows in the Nordic seas*

*Julia Smirnova, Pavel Golubkin*

The ongoing research is dedicated to assessment of threats that polar lows pose to maritime activities in the Arctic. The polar lows are extreme weather phenomena that characterized by storm winds and form at high latitudes in both hemispheres over ice-free sea surface. In the first stage surface waves generated by polar lows were assessed in the Greenland, Norwegian, and Barents seas for 1995-2009.

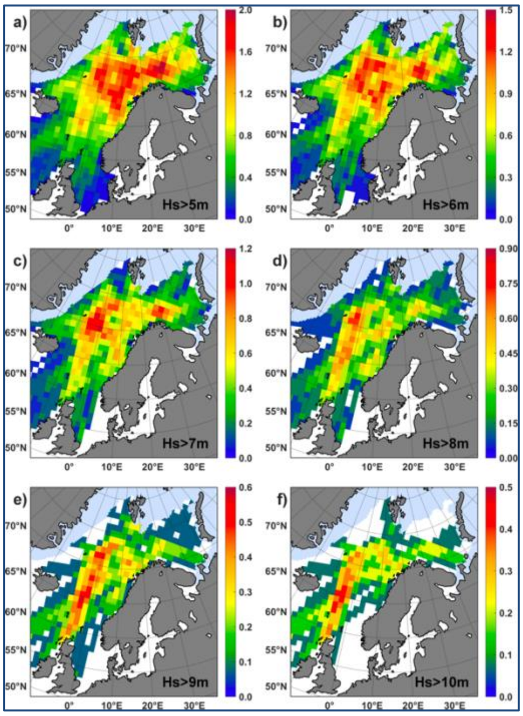


***Figure 2.*** *Spatial distribution of polar low generated waves exceeding given height. Shades correspond to frequency per year in 100×100 km cells. Light blue area represents median sea ice extent for study period.*

For this purpose, a previously developed polar low climatology and a simplified model of wind wave generation by a moving cyclone were used. Wave heights for every cyclone were calculated using mean cyclone directions, connecting first and last point on trajectory of every polar low. Accounting for the width of polar low mean wind speed profile, it was assumed that the wave generation occurs in the right sector of a cyclone in a band from 0.1 *D* to 0.35 *D*, where D is polar low diameter. After the end of polar low lifetime, waves continued to travel in the direction of polar low movement as swell until they reached coast line, ice or escaped from the analysed region.

Fig. 2 shows the spatial distribution of waves exceeding a given height for the Greenland, Norwegian, and Barents seas as frequency per year in 100×100 km cells. As follows from the figure, spatial distribution of the medium height waves (5-6 m) approximately corresponds to the spatial distribution of genesis areas of polar lows themselves. They are often observed in the whole analysed region; frequency is approximately from one to almost two cases per year in most cells. Apart from the Kola Peninsula, these waves may be equally often observed in all coastal areas. Higher waves are most frequent in the Barents Sea northeast from the North Cape, and in the western part of the Norwegian Sea. Frequency of waves larger than 8 m in these regions is approximately one case every two years. Emergence of waves larger than 8-10 m is also possible in coastal regions, although more rarely – about one case in five years.

### *Changes in sea ice volume in the Greenlanad, Irminger and Labrador seas between 1978 and 2016*

*Valeria Selyuzhenok, Igor Bashmachnikov, Aleksandra Mushta, Leonid Bobylev*

Deep convection in the Greenland, Irminger and Labrador seas is an inherent part of the Atlantic Meridional Overturning Circulation (AMOC), which modulates its intensity. Interannual variations in the intensity of deep convection, among other factors, are thought to be controlled by variations in the intensity of freshwater fluxes to these regions and the overall sea-ice extent in winter.

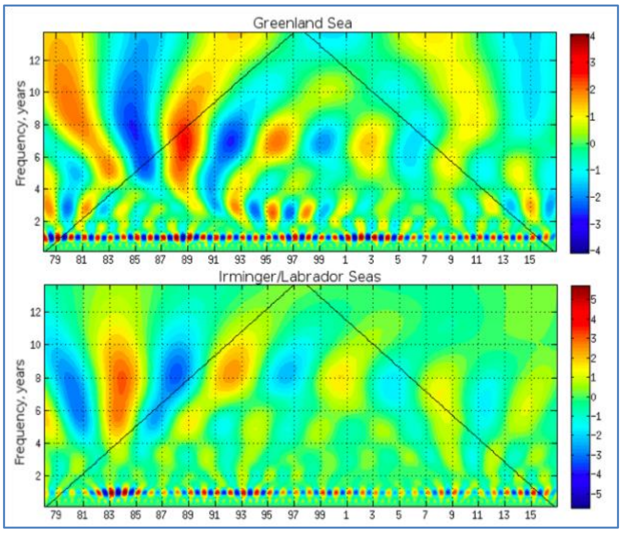


***Figure 3.*** *Results of wavelet analysis of winter sea ice volume time series (trends excluded).*

Here we present the analysis of interannual and annual sea ice volume variations in the Greenland, Labrador and Irminger seas between 1978 and 2016. The time series of sea ice volume were taken from Pan-Arctic Ice Ocean Modelling and Assimilation System (PIOMAS). Data present monthly mean sea ice volume on a model grid, which is re-projected to 25EASE-2 grid. We extracted monthly sea ice volume data for two regions: Greenland Sea and Irminger and Labrador seas. Analysis showed a statistically significant trend towards reduction of integral winter (January-April) sea ice volume with the speed of 14.3 $km^3$ per year in the Greenland Sea. The Irminger and Labrador seas winter sea ice volume appears to have no statistically significant changes during the studied period. A wavelet analysis was performed in the order to reveal periodic variation of sea ice volume in the regions (Fig. 3). The analysis revealed variation of sea ice volume with periods of 3 and 6-8 years in the Greenland Sea and 8-10 years in the Irminger and Labrador seas. The 6-8-year cycle in the Greenland Sea lags between a quarter and a half of the period of corresponding variations in the Irminger and Labrador seas. These variations are in the agreement with the Arctic Oscillation Index. However, this linkage requires further investigation.

## Aquatic Ecosystems in Response to Global Change

### *E. huxleyi blooms influence on carbon cycle*

*Dmitry Kondrik, Dmitry Pozdnyakov, Eduard Kazakov, Lasse Pettersson*

The main aim of this study was to evaluate the influence of vast *E. huxleyi* blooms on the carbon cycle in the atmosphere-ocean system. On a basis of our previous results from bloom delineation process in North, Norwegian, Greenland, Barents and Bering seas three significant steps were performed. The first step was to evaluate the total amount of Particulate Inorganic Carbon (PIC) produced by each bloom during every year, the second step was to estimate $CO_2$ partial pressure increase *($\Delta pCO_2$)* due to bloom presence. Finally, the third step consisted in assessing the increase in $CO_2$ partial pressure in the atmospheric column over the blooming area.

In the first step, initially identification and delineation of target blooms were performed using a triple approach: the radiometric properties of bloom areas and the spectral composition of remote sensing reflection, Rrs, were conjointly used and paired with the data on the location of the isoline of some threshold coccolith concentration, $C_{cc}$. $C_{cc}$ values were retrieved also from Rrs with a multispectral optimization algorithm based on the Levenberg-Marquardt multivariate optimization technique. Thus, the use of the above three advanced approaches assured a truly confident bloom area delineation. From $C_{cc}$ data, PIC assessments were performed. Together with the bloom area data, the PIC results were jointly analysed to reveal the dynamics of the E. phenomenon for the whole period of study, i.e. 18 years.

In the second step, an innovative algorithm was developed to calculate the so-called background $pCO_2$ values at 10°C within the target area prior to the onset of *E.* blooming. These results were further used to quantify the spatial variations of $\Delta pCO_2$ in the North, Norwegian, Greenland, Barents, and Bering seas over 18 years. The analysis was performed conjointly with the above time series of PIC and bloom area *S*.

In the third step, spaceborne data on atmospheric columnar $CO_2$ partial pressure were employed to assess the effect produced by *E.* blooming on this parameter. This was done over the Black Sea, which was taken as an example as this sea is known for its basin-wide blooms of this microalga.

Analysis of obtained results have shown that *E.* blooms in the North Atlantic and Arctic seas generally occurred annually across 1998-2015, although the extent of blooms varied appreciably from year to year. Through the above years, maximum bloom area *S* in the target seas in some specific years was also very significant. Thus, for all target seas, the bloom area ratio to the total sea area varied from 4.8% (Greenland Sea) to 23.7% (Barents Sea).

Although no tendency in interannual variations of the bloom area and blooming duration was found, the pattern of temporal variations in S exhibits some salient features: (a) were years of particularly vast blooms that interlaced with periods of smaller blooms; (b) years of occurrence of spikes in S were different for the target seas; (c) the intermissions between the spikes for the North, Norwegian, Greenland, and Barents seas showed no periodicity so that no apparent regularity is observed.

In contrast to the target North Atlantic and Arctic seas, the bloom activity in the Bering Sea exhibited a very specific sequence: there was a period between 1998 and 2001 of very high blooming activity that was followed by a drastic drop in both the number of occurrences and the extent of *E.* blooms. The only exception was found for 2014 when a moderate spike in S took place. This specific feature inherent in the Bering Sea also shows that in the years of anomalous high blooming activity (1997/1998–2001) its annual duration reached 10 months, whereas in the North Atlantic seas it did not exceed ~1.5 months.

A similar pattern was observed for the PIC maximum production within *E. huxleyi* blooms: 0.4 kt-0.14 Mt in the Greenland Sea and ~0.35Mt in the Barents Sea. As for the *E.* bloom areas in the Bering Sea during 1997-2001, they are rather similar with those of the Barents Sea. However, the PIC production in the Bering Sea appeared to be higher than in the Barents Sea by a factor of two, with maximum values reaching 0.4 Mt and, in one case (in 2001), even ~0.7 Mt.

*$pCO_2$* increments determined in surface waters within *E.* blooms in the target seas and normalized to respective background *$pCO_2$* values *$(pCO_2)_b$* are found to be sea- and year-variable (Fig. 4): the mean maximum and maximum values of normalization result within the *E.* blooming area and over 18 years of observations varied in percent in the target seas between 21.0-43.3, and 31.6-62.5,

respectively, with the highest and lowest values belonging to the Greenland and Barents seas. The time series of $\Delta pCO_2/(pCO_2)_b$ maximum values through 1998-2015 do not exhibit any discernible trends but show a rather irregular pattern with intermittent periods of enhanced and

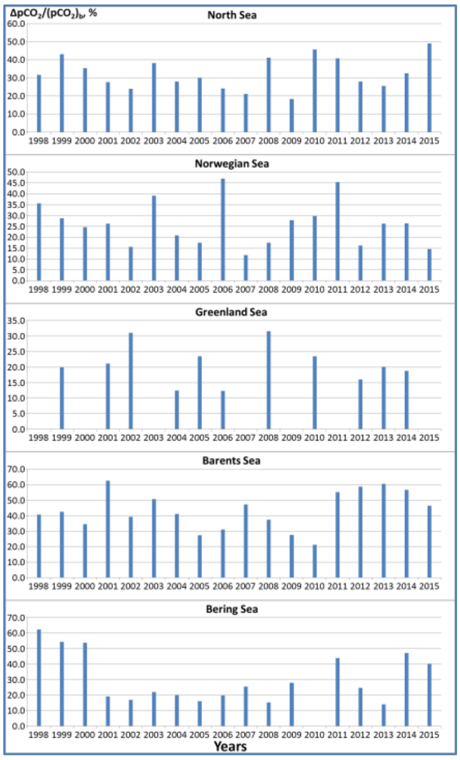


***Figure 4*** *Spatial and temporal variations in $[\Delta pCO_2/(pCO_2)_b]\cdot 100\%$ maximum values within E. huxleyi bloom areas in the North, Norwegian, Greenland, Barents, and Bering seas during 1998-2015. Note: data are absent for some years and target seas as the respective $\Delta pCO_2$ values proved to be lower the assessed.*

relatively subdued peaks.

These quantitative assessments have explicitly shown that vast *E.* bloom areas can indeed play significant role in the exchange of carbon between the atmosphere and the ocean. Indeed, the actual influence of *E.* blooms on $CO_2$ partial pressure in sea surface water should also be considered in terms of the phenomenon duration. The bloom duration (*t*) of this alga in the target seas in the North Atlantic and Arctic is within 30-50 days, whereas in the Bering Sea during the years of 1998-2001 it was up to 270-300 days, that is, this impact is not short living but contrarily rather long lasting. Besides, the importance of the effect could be also assessed via the cumulative bloom area ($\Sigma S$) throughout the vegetation period across all target seas. Thus, for the studied seas $\Sigma S$ proved to be within the range of about 220-565 hundred thousand km$^2$, that is, constituting a very significant part of the water surface considered in our study. Given that the *E.* blooms in the Northern Hemisphere regularly occur in a larger number of seas, the overall value of $\Sigma S$ is in the reality far higher. This phenomenon proves to be omnipresent across the global oceans. Moreover, the collective area of *E.* in the Southern Hemisphere is reported by about 1.5 times larger than in the Northern Hemisphere. Thus, globally the effect of weakening of marine carbon sinks due to coccolithophore blooms might be appreciable, and remote sensing offers the ability to assess the *E.* blooming consequences for worldwide marine environments.

An explicit evidence of the above considerations was obtained over the Black Sea. The registered *E.* blooms in the Black Sea in 2015 and 2016 (Fig. 5a) occurred during the period extending roughly between late April and late June with the maximum bloom area developing in mid-May. Our quantitative assessments of the *E.* bloom extent in the target sea indicate that we deal with a huge phenomenon. Indeed, as Fig. 5a illustrates, both in 2015 and 2016 the bloom areas at the stage of maximum development reached 180-200 thousand square kilometres, e.g. nearly half of the total surface of the Black Sea. For both periods of blooming, the concurrent OCO-2 data are reasonably ample. Variations in $XCO_2$ over the Black Sea (Fig. 5b) exhibit a characteristic seasonal pattern with high and low values, respectively, in winter and summer, which is in accordance with the global data.

Fig. 5c represents the results of application of the procedure of polynomial approximation to all $XCO_2$ values illustrated in Fig. 5b (green curve), and only $XCO_2$ values registered beyond the period of blooming (red curve). These two data sets reveal enhanced values of the column-averaged volume mixing ratio of carbon dioxide $XCO_2$ over the bloom areas. Calculated as the difference between mid-box and respective red curve $XCO_2$ values, the magnitude of $XCO_2$ increment for both years proved to be appreciable: the maximum increments of $XCO_2$ are close to 2 ppm (Fig. 5d), i.e. about 2 µatm, which constitutes ~0.5% of the contemporary mean $pCO_2$ in the atmosphere. Thus, the increcement established in this study should generally be considered as reliable.

*Acknowledgment: this study was conducted under the Russian Science Foundation financial support (project No. 1717-01117).*

*Relevant publications: Kondrik, D., Pozdnyakov, D., & Pettersson, L. (2017). Particulate inorganic carbon production within E. huxleyi blooms in subpolar and polar seas: a satellite time series study (1998-2013). International Journal of Remote Sensing, 38(22), 6179-6205.*

*Kondrik, D., Pozdnyakov, D., & Johannessen, O.M. (2018). Satellite evidence that E. huxleyi phytoplankton blooms weaken marine carbon sinks. Geophysical Research Letters, 45(2), 846-854.*

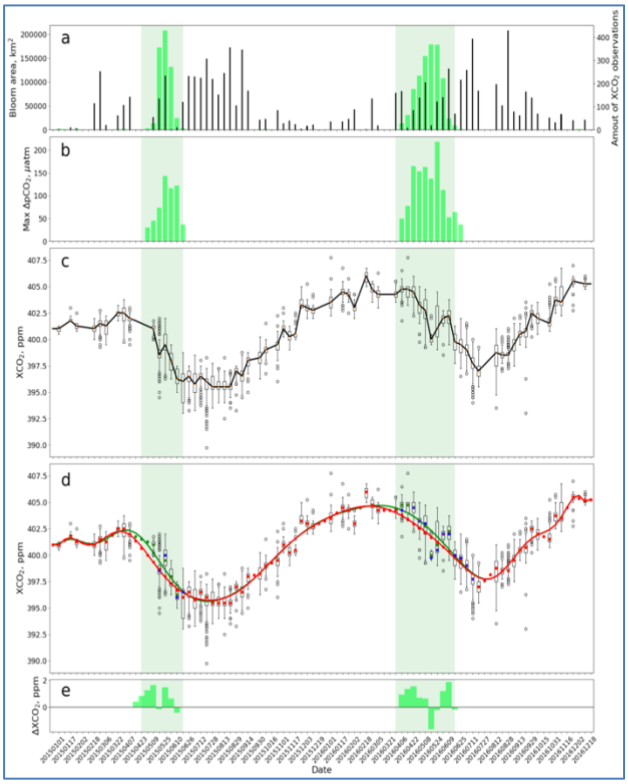


***Figure 5*** *Phenomenon of E. huxleyi blooms in the Black Sea in 2015 and 2016 as observed from space: **(a)** bloom area (green bars), and number of $XCO_2$ observations (black bars); **(b)** $\Delta pCO_2$ maximal values in water within bloom area (green bars); **(c)** intraannual variations of $XCO_2$; **(d)** polynomial approximations of $XCO_2$ values illustrated in panel (c) (green curve), and $XCO_2$ values registered beyond the period of blooming (red curve); **(e)** $XCO_2$ increments over bloom areas. Pale green columns in (a-e) reflect period of blooming. Other designations: boxes and thin vertical black bars show range of $XCO_2$ values constituting, respectively, 50% and 49.3% of entire number of $XCO_2$ retrievals; open black circles show the rest 0.7% of $XCO_2$ values that are beyond above ranges; red and green filled circles show medians for two cases illustrated in panel (d) (colour relates to colour of curves in panel (d)).*

## Bio-optical retrieval algorithm for the optically shallow waters of Lake Michigan

*Anton Korosov, Artem Moiseev, Dmitry Pozdnyakov*

We developed an original approach to the optical-optical multi-sensor image fusion. Here we used multispectral images from Sentinel-2 and RGB images from MODIS. The images from both sources related to one and the same area and time of data acquisition. It was purported to provide a visually easily perceivable result of fusion. A statistical assessment of correspondence between remote sensing reflectance (*Rrs*) values inferred from the MODIS and fused data at three wavelengths used to generate the RGB images was intended to illustrate the fusion procedure adequacy.

The developed approach is based on

application of the neural network emulation technique coined here as artificial neural network (ANN). In application to image fusion, the ANN-based method employs a nonlinear response function that iterates many times in a special network structure in the order to learn the complex functional relationship between input and output training data.

As the above approach was applied to optically shallow waters of Lake Michigan, it was complemented by fuzzy k-mean classification algorithm for bottom type identification. The important advantage of such algorithms is that they can be employed under conditions of a near-complete absence of information on the type of data distribution.

The Multispectral Imager (MSI) on Sentinel-2a provides data at high spatial resolution (10-60 m) in several spectral channels in the visible. However, the number of spectral

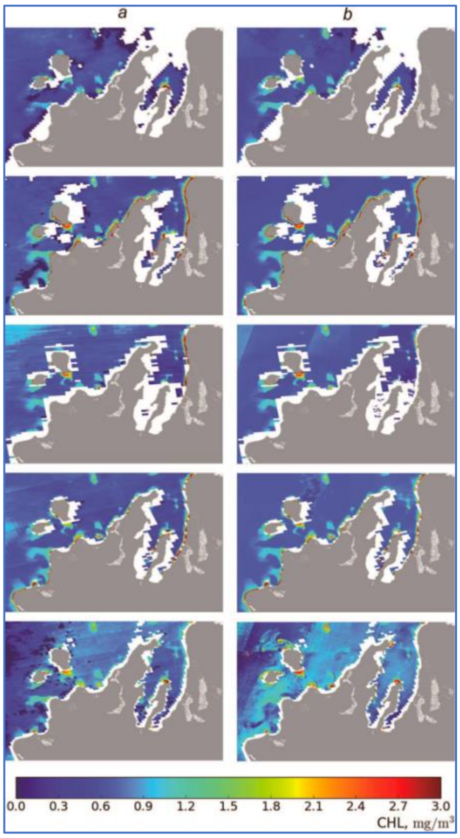


***Figure 6.*** *Spatial distributions of phytoplankton chlorophyll from **(a)** MODIS-Aqua data; and **(b)** fused MODIS-Aqua and Sentinel-2a data for 09.05, 05.07, 26.07, 15.08, 04.09 2017 (presented in the top to bottom sequence).*

channels in the visible (only four) and their placement are, respectively, rather limited and not optimally suited. These deficiencies preclude the use of this sensor for efficient retrieval of water quality parameters in situations of optically complex or shallow waters. Thus, in our studies MSI acted in the capacity of a sensor with high spatial resolution (60 m) but low spectral resolution (only 4 bands in the visible), i.e. its data were to be fused with a sensor providing higher spectral resolution although at a rather coarse spatial resolution. As such, data from MODIS-Aqua were used: they are available at a much higher spectral resolution (6 bands in the visible and 1 band in the near IR), but at a lower spatial resolution (with 1 km in the visible). Analysis of MODIS-Aqua data to be conjugated/fused with Sentinel-2a data has shown that the NASA embedded atmospheric correction was unsatisfactory, and to overcome this problem, we applied the MUMM code.

In the developed algorithm, the ANN consists of four layers of neurons. The RGB images developed from fused Sentinel-2a and MODIS-Aqua data exhibit a logical sequence of phases of phytoplankton development in Lake Michigan. Indeed, the green areas (corresponding to enhanced concentrations of phytoplankton chlorophyll) stand out twice in the year, viz., in spring and early autumn, which is in complete conformance with vernal and autumnal phytoplankton outbreaks in Lake Michigan. To retrieve the concentration of phytoplankton chlorophyll from the two sorts of spaceborne data, the BOLEALI-OSW algorithm was utilized. Fig. 6 illustrates the spatial distributions of phytoplankton chlorophyll concentrations for the five dates as obtained from the fused MODIS-Aqua and Sentinel-2a data. The paired plates in Fig. 6 explicitly show the advantage of the fusion procedure over the results from solely MODIS-Aqua.

Mapping of bottom type was performed for an area called Pyramid Point within the Sandy Bear Dunes site. The k-means technique was applied to bottom substrate classification. Spectra of *Rrs* values from the fused data (at 60 m resolution) were partitioned into three classes: sand, Chara stands, and some sandy substrate either sparsely covered by macrophytes Chara or Cladophora or slightly silted. The area was confined to depths not exceeding 15 m.

The clusterization thus performed permitted to produce a map of bottom type heterogeneity at a 60-m spatial resolution. The above-described bottom type classification reveals that the area adjacent to the coast is sandy. Further off-coast, the area with a depth of 10-15 m is covered by Chara stands. The intermediate area belongs to the intermediate class, although it contains sandy spots as well as spots covered by submerged vegetation stands. These features explicitly indicate that the spatial heterogeneity of the area ascribed to class 2 is not due to depth changes but is driven by changes in the bottom albedo.

Thus, summing up, developed and realized in a computer code our own method of ocean colour data fusion, and the possibility of employing the fused data for retrieving the bottom type investigated. The attained results strongly suggest that the developed algorithm can be successfully used for fusion of data from Sentinel-2 and Sentinel-3 because Sentinel-3 is highly akin to MODIS-Aqua in terms of the spectral and spatial resolution.

Relevant publication: *Korosov, A., Moiseev, A., & Pozdnyakov, D. (2018). Modis-Aqua and Sentinel-2 data fusion: application to optically shallow waters of Lake Michigan. Limnologia, doi: 10.17076/lim692.*

## *Spatial data assimilation with a service-based GIS infrastructure for mapping and analysis of E. huxleyi blooms in the Arctic seas*

*Eduard Kazakov, Dmitry Kondrik, Dmitry Pozdnyakov*

A coccolithophore *E. huxleyi* is one of the most significant sources of inorganic carbon in the world oceans. Forming vast bloom areas this species can affect the carbon balance in the atmosphere-ocean system, and thus interfere with climate and marine ecology. A 19-year time series (1998-2016) of spaceborne data on this phenomenon from 6 seas located at high latitudes as well as data on the phenomenon-affecting oceanographic and atmospheric variables were collected. These data were collected from the following spaceborne sources: Ocean Colour Climate Change Initiative (OC) portal, AVHRR, ASCAT QuikSCAT, OCO-2, and SSM/I. Apart from the above listed spaceborne data, our study required the data on water salinity, availability of nutrients (such as nitrates, phosphates, and silicates) and mixed layer depth. These data were available from The GLobal Ocean Data Analysis Project (GLODAP) database, The SOCAT database (The Surface Ocean $CO_2$ Atlas), World Ocean Atlas 2013 (WOA13, NOAA). The variety of data complicates their joint processing and collocated interpretation. One of the most important steps in such a study is the space-time assimilation of all data, bringing it to a single standardized form. The 8-day composites available from the OC portal were used as basic data, accordingly all other complementary data were brought to the same time resolution. As a spatial domain, a 2500×2500 grid was chosen at a spatial resolution of 4 km within the limits between 5000000 and 5000000 on both coordinate axes in the Lambert azimuthal equal area projection called NSIDC EASE-Grid North (EPSG: 3973). All data sets were recalculated into this domain with special software modules. To efficiently concatenate and eventually analyse such versatile data of huge size, a special GIS infrastructure (GISI) is developed. It is built on the principles of a service-based architecture with micro-services. The GISI includes both a server application that controls information flows and automated data processing.

Given both the variety of complex and heterogeneous data to be processed and analysed in the study, and the need to continuously update the baselines of data and perform new calculations of the thematic products, there arise the problem of developing an integrated software infrastructure that complies with the following tasks: (i) automation of new data uploading; (ii) assimilation of data into a single space-time domain; (iii) unified storage of data; (iv) automation of calculations of the basic thematic products; (v) providing user interfaces for the retrieval of and access to the desired data; (vi) providing mechanisms for making calculations outside the infrastructure; (vii) providing opportunities for standardized visualization of data in GIS, preparation of reports and maps.

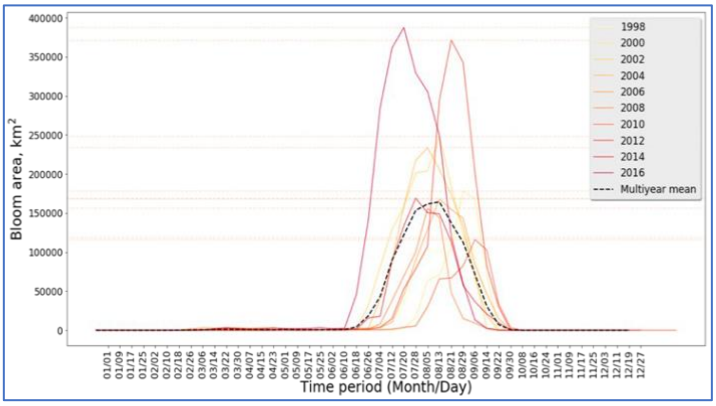


***Figure 7.*** *Spatio-temporal statistics of blooms in the Barents Sea.*

Unforeseen requirements for the infrastructure scaling in the future, as well as the overall complexity of the tasks to be performed, make it necessary to look for modern approaches. To date, the popular versions of the architecture of scientific information systems are those built on the principle of micro-services within a server-oriented architecture. With this approach, each separate functional block of the software infrastructure is an independent service performing an atomized task, accepting a standardized query, and generating the result in the same standardized representation, while the internal mechanisms of its operation are hidden from the user.

The information system developed in this study bases on a two-layer architecture: for the user, the kernel of the system works as a server application that processes various requests received via the HTTP protocol in accordance with the REST concept. Inside the server part, all interactions take place at the level of micro-services that perform tasks in the following categories: (a) data storage; (b) storing of and searching for metadata; (c) data downloading from remote servers; (d) preliminary preparation of data, their spatial-temporal assimilation; (e) thematic processing of data, calculation of derivative products.

Using micro-services allows to effectively manage the infrastructure, complement new necessary blocks to it without affecting other parts of the system. This approach justifies itself in the case of merging of new data sources, improvement of mechanics of preliminary and thematic processing, potential emergence of new tasks related to other data and instruments.

Interaction with such an infrastructure for user can be implemented from any convenient environment through HTTP-requests. For convenience and the solution of standard tasks, three basic user interfaces for data access were developed: (1) NIERSC Data Centre - web portal; (2) extension for the open-source desktop geoinformation platform QGIS; and (3) a library for the Python, which provides access to the server kernel functions from the user programming code. Such a three-sided approach to user interfaces realization performs well and seems to be a full-fledged decision to provide a variety of tasks.

Some basic results of using such an infrastructure, can be illustrated with the zonation of coccolithophores activity in the Barents Sea performed on basis of a set of blooms data covering mentioned above 19-year period (see Figure on the cover page of this report). The Barents Sea is a right representative of stably blooming water areas. The spatio-temporal characteristics of the bloom in different years are shown in Fig. 7. Obviously, significant interannual variations are observed in both the intensity of blooms and in their time ranges. Also, the localization of most frequently occurring bloom areas are of great interest.

*Acknowledgment: this study was conducted under the Russian Science Foundation financial support (project No. 1717-01117).*

# Applied Meteorological and Oceanographic Research for Industrial Activities

## *Integrated satellite ice monitoring in the Kara and Okhotsk seas for supporting industrial activities*

*Vladimir Volkov, Natalia Zakhvatkina, Eduard Kazakov, Denis Demchev, Stein Sandven; Eduard Khachatrian, Elena Shalina, Aleksandra Mushta, Kirill Smirnov*

The Nansen Centre had developed a logistic model for providing scientific and operational information, products and services to potential users, which is necessary for planning of prospecting and drilling works and management of ice operations on the shelf of the Arctic seas, and ensuring ice and environmental safety.

The key block of this system is the Geoinformation Automated System of Satellite Ice Monitoring of the Nansen Centre (GASSIM-NC), which includes original methods for processing satellite (mainly radar) data to obtain maps of sea ice distribution by age, ice drift and deformations (compression-rarefaction), especially dangerous ice formations and phenomena. The ice conditions analysis methods developed at the Nansen Centre are constantly being improved. The system is "open" to connect similarly configured climatic and environmental blocks.

Complex tasks, including both the provision of scientific analysis and the supply of operational data, determine the need to create a single information space that would combine data flows, their processing and presentation. Such system addresses the following main objectives: (i) provision of continuous automatic collecting and archiving satellite data; (ii) storage and presentation of these data in standard GIS-formats, provision of access to them by means of different interfaces, also in the Internet network; (iii) thematic data processing; (iv) publication of thematic products in standard GIS-formats, provision of their operational delivery to users; (v) provision of functional and convenient set of tools for data loading and processing.

Approach for developing GASSIM-NC and its infrastructure are the same as those described above in the section "Spatial data assimilation with a service-based GIS infrastructure for mapping and analysis of E. huxleyi blooms in the Arctic seas".

Interaction with such an infrastructure for user (researcher) can be implemented from any convenient environment through HTTP-requests. For convenience and the solution of standard tasks, three basic user interfaces for data access were developed: NIERSC Data Centre - web portal; extension for the open-source desktop geoinformation platform QGIS; a library for the Python (see above).

Another component of the system is experimental desktop with virtual environment for client-side data processing. Sharing such virtual machines based on Vagrant and Oracle VirtualBox software can be effective solution for the independent processing with client's computing resources.

During last year, system was evolved: algorithms for sea ice classification and drift retrieval were assimilated, more than 15000 SAR scenes were archived and pre-processed, scenes for sea ice monitoring purposes were selected.

In 2017, the system was used in the framework of contracts with FRECOM Ltd for information support of some industrial companies operating in the Kara and Okhotsk seas. All calculations were carried out using advanced methods adapted to these water areas and based on a single stream of satellite information. As a result, sea ice maps were created in GIS-formats in accordance with the requirements of the customer. Analysis of ice conditions for the number of recent years was carried out "on the background" of the results of analysis of long-term changes in the ice regime.

Using GASSIM-NC, the processing and analysis of the satellite information was carried out in several thematic areas.

**Automatic classification of sea ice cover.** Currently the most optimal way for the sea-ice cover monitoring is the utilizing of a high spatial resolution satellite radar images acquired from Synthetic Aperture Radars (SARs). Using these images, the automatic

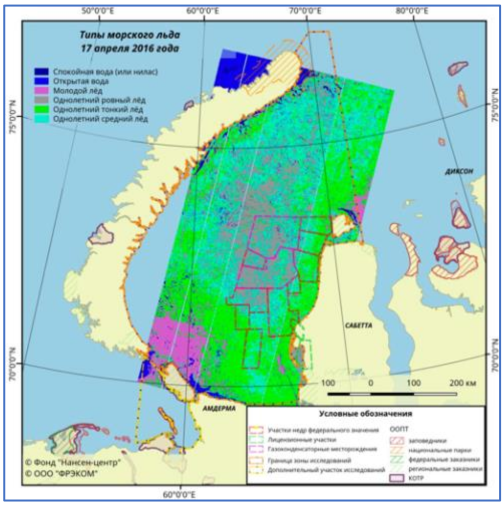


*Figure 8. Performance of sea ice classification algorithm for the Kara Sea, 17 April 2016.*

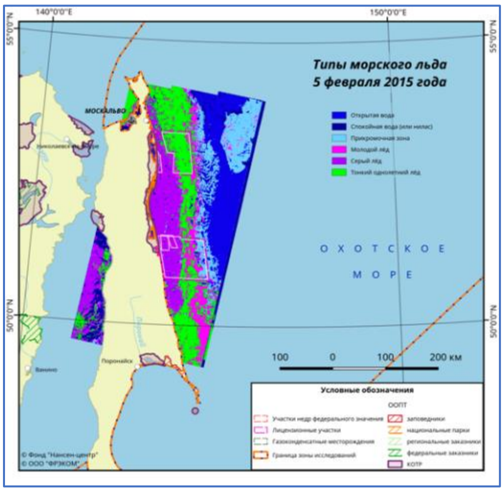


*Figure 9. Performance of sea ice classification algorithm for the Okhotsk Sea, 5 February 2015.*

sea-ice classification algorithms were applied as a part of an integrated system for the satellite information processing.

Within FRECOM projects, previously elaborated algorithms for mapping ice and water surfaces and obtaining ice type classes using RADARSAT-2 images were adopted and improved to detect ice types and water surface using Sentinel-1-Wide (EW) swath mode data.

In the Sentinel-1 image the HV polarization of EW mode is formed from narrower bands, that causes the visible modulation of the image intensity in the range direction (thermal noise effect). In the HH-polarization image, sea ice backscatter coefficient of the same ice type is varying with the incidence angle and the corresponding difference can reach significant values, especially for the windy open water surface. The techniques for compensation of these effects were developed.

The ice type classification is carried out by implementation of the Support Vector Machine method (SVM). Learning classification requires training samples to obtain class statistics. The ice experts perform a visual analysis of the SAR data with selected ice types and water samples for training and testing the classification. To improve the separation of the classes the training vectors of the classifier are formed from data obtained with the texture analysis.

Algorithm is trained for the Kara (Fig. 8) and Okhotsk (Fig. 9) seas and is able to distinguish several classes: first-year ice (FYI) medium, FYI thin, young ice (with grey ice detection in the Okhotsk Sea), some very smooth (level) FYI, and open water – calm and windy. Also, a Marginal Ice Zone (MIZ) – rather narrow area between open water and ice, which, in general, consist of the same ice type as the main closed ice area with more younger ice and some forms of broken ice – can be detected in the Okhotsk Sea. The algorithm versions could not recognize the fast ice. Also, the multiyear ice was not considered in these areas. The final step was to provide a classified SAR image in the GeoTIFF format in terms of WMO palette conditions.

Ice types and open water recognition algorithm in the most cases gives stable satisfactory results. On the received charts, it is possible not only to highlight a border between ice and water and detect the ice zones, but also to obtain information about irregularities such as large cracks and leads.

**Method of drift and deformation fields retrieval.** There is ongoing development of ice drift retrieval algorithms from radar images at NIERSC. The physical features of radar backscatter signal from ice surface manifest in specific brightness variability from pixel to pixel and called speckle. This undesirable effect has to be considered closely to improve ice drift retrieval performance. Therefore, suppression of speckle is the main goal of SAR image preprocessing stage. Along with averaging of independent signal of the same object – multilooking, spatial methods of SAR image filtering may be useful for the successful image interpretation.

Another challenging issue requiring special attention is the accuracy of resultant ice drift vectors. It is known that the error of just 100 m in ice displacement determination may lead to the error in ice deformation estimation of the same order. Hence, a special attention should be paid to this problem too for successful ice kinematic analysis.

In 2017, several case studies in the Western Arctic have been performed to evaluate the efficiency of different noise suppression and feature tracking techniques. The results showed high potential of anisotropic diffusion based methods for SAR image processing. The state-of-the-art methods have been compared in terms of spatial data density, accuracy and time efficiency. Anisotropic diffusion technique exhibits the best compromise between tracking performance and execution time (Fig. 10).

**Method for identification and monitoring of icebergs and other dangerous ice formations.** To reveal the true regularities of the seasonal and interannual variability of the number of icebergs in the Arctic it is necessary to use remote sensing data and automated approaches to iceberg detection. Thus, images of Sentinel-1 were employed to implement this task.

Based on the developed automated method of iceberg detection, a test analysis of the seasonal and interannual variability of the number of icebergs in the area of the Barents Sea was performed. For the test calculations and the regional analysis of regularities in the iceberg distribution, the site in the Barents Sea was chosen to the west of the Novaya Zemlya Archipelago. As a result, a total of 765 dots on 51 images were detected, which could very likely correspond to icebergs (Fig. 11).

For a statistical description of the spatial distribution of icebergs the study region was divided into 16 cells with equivalent area. An obvious non-homogeneity of the spatial distribution of icebergs is noted over the region (see Fig.11): their maximum number (about half) is observed in the cell A2 and in adjacent cells – A1, B1, B2 where their number is also high – 85, 70 and 53, respectively; thus, 75% of all detected iceberg-typical dots, is concentrated here.

Our study allowed to make for the first-time conclusion on the interannual and seasonal variability of the number of observed icebergs (Fig. 12). There is an obvious

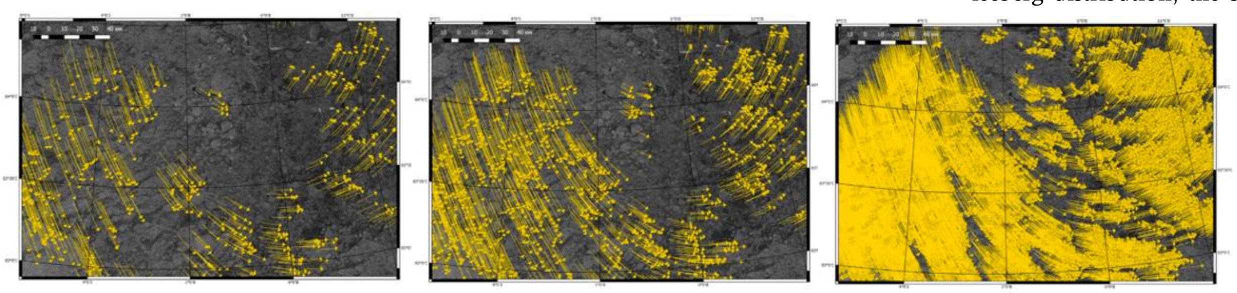

*Figure 10. A comparison study of various filtering techniques for ice drift retrieval from Sentinel-1 images in the Fram Strait: **(left)** no filtering; **(centre)** SIFT (Gaussian kernel); **(right)** Anisotropic Diffusion Filter.*

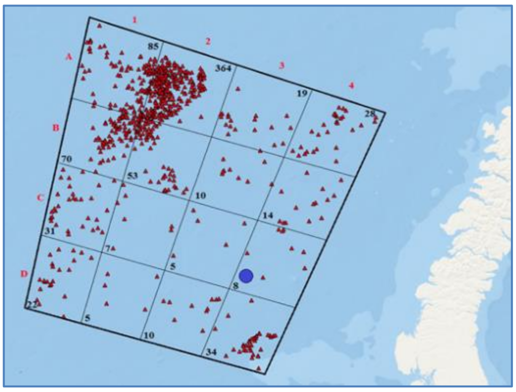

*Figure 11. Spatial distribution of icebergs in the central region of the Barents Sea. Blue circle denotes location of the Shtokman field. At the corner of each cell, the number of icebergs detected within it is given. Letters and numbers denote lines and columns of cells with equivalent area.*

general tendency for the increase of their number in the winter hydrological season and the decrease in the summer season.

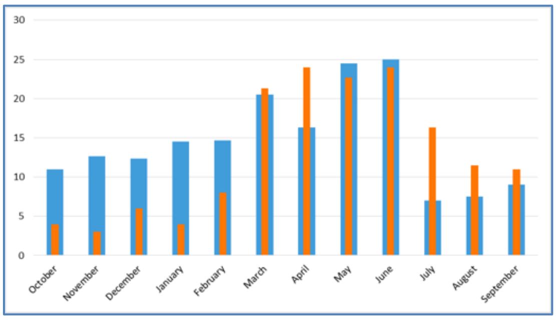


*Figure 12. Seasonal and interannual variability of the number of icebergs. Red color shows data for the period October 2014 to September 2015, blue color – from October 2015 to September 2016.*

**Analysis of long-term changes of ice regime in the Kara and Okhotsk seas.** Sea ice variability and change in these seas over the period 1979-2015 have been analysed using satellite passive microwave measurements (see NSIDC web site). It is known that both Kara and Okhotsk seas significantly contribute to the sea ice decline in the Northern Hemisphere correspondingly in summer and in winter.

***Kara Sea.*** The Kara Sea has been totally covered by ice in winter in most of the years in the period 1979-2015. Meanwhile, in the recent years some record sea ice minimums have been observed in winter, with the lowest in March 2012, when the south-western part of the sea was partly ice-free and partly covered by the young ice. The near surface temperature in that region during March 2012 was 4-6 degrees above the average and in the following September the overall extent of the Arctic sea ice reached its all-time low.

The process of sea ice destruction in the Kara Sea starts in June and enhances in July. Sea ice minimum is usually observed in September. During the last century sea has totally cleared from ice in summer only once, in 1995. In other years in 1979-2000 in summer sea was partly covered by ice, up to 50% of the whole sea area. In present century, we witness the tendency of appearing larger ice-free areas or totally ice-free sea. The average sea ice area observed by satellites in September in the Kara Sea was 24% of the total sea area in the period 1979-1999 and about 8% in 2000-2015; the overall decline loss is 6400 km$^2$ per year. The variability of sea ice area is very high: the standard deviation amounts to 199 km$^2$ being 88% of the average sea ice area in September.

During 2014-2017 ice conditions in the Kara sea in summer were not too complicated compare with the climatic norms. In these years, the steady ice formation in the northern part of the Kara sea began in the first decade of September, in the southwestern part - in October, on open water in the absence of residual ice. In the last 5 years freezing began in October among the residual ice; the ice formation isochronous was directed from the northeast to the southwest. Ice accumulations appeared near the Northern Earth and blocked the Vilkitsky Strait (2013, 2014). In 2014, these ice fields were a continuation of the Arctic drifting ice field. In October 2012, 2015 and 2016 sea was free of ice; ice border was leaving behind 82° east. Freezing of the ice took place on the open water, in the absence of residual ice of any cohesion and form.

In general, it is possible to group winters with a similar development of ice cover: (i) 2012-2013 and 2016-2017; (ii) 2013-2014 and 2014-2015. The first group is characterized by a long preservation of open water and rapid freezing in January with predominance of gray-white ice and a tongue of thin ice penetrating from the north-eastern part of the sea. The second group is characterized by freezing the rest of the open water in the south of the sea in January and dominating of the thin ice. In 2015 along the coast of Novaya Zemlya the thick ice was formed.

According to the average long-term data, the steady melting of the snow-ice surface of the Kara Sea begins in the region of the Amderma coast in the 3rd decade of May. In the last 5 years, the process of cleansing the sea from ice began earlier - in April-May, with melting points of rivers mouths and the Kara Gates Strait. Cleansing the Kara Sea from ice can pass both from east to west, and from the west to the centre of the water area.

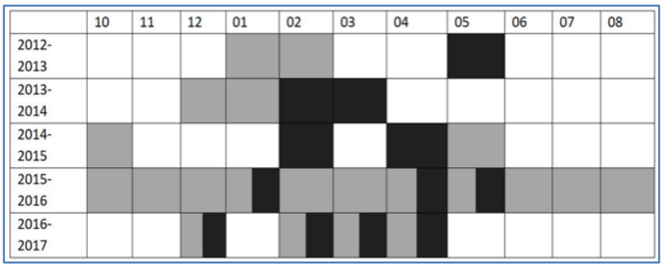


*Figure 13. The presence of polynyas in the Kara Sea in the winters of 2012-2017 (black cells - along the Novaya Zemlya, grey ones - at the cape of Zhelaniya).*

One of the features of the Kara Sea ice extent is the polynyas along the Novaya Zemlya and north of cape of Zhelaniya, which periodically appear and disappear. The time of existence of these polynyas is shown in Fig. 13. Frequently the Novaya Zemlya polynya occurs in February, can last two months (2014) and finally can disappear and appear again in April (2015, 2016). In 2013, there was no Novaya Zemlya polynya during the winter; it appeared only in May and its appearance caused a rapid ice melting. In 2017, on the contrary, the polynya appeared in December, disappeared until February, then appeard again and existed until the sea was fully free of ice.

Polynya north of Novaya Zemlya appeared in winter 2012-2013 in January and lasted until March, in 2013-2014 it appeared in December-January, in 2014-2015 – in October and May, in 2015-2016 – in January and lasted the whole year, in 2016-2017 – in December.

In the last two years there has been a tendency towards a decrease of fast ice area in the Kara sea.

From 2011 to 2015 the main directions of ice drift were the northeast (23%), north-north-east (22%) and north-west (8%); see Fig. 14. In relation to Novaya Zemlya, several types of drift, occurring in the southwestern part of the Kara Sea during the winter season, can be distinguished: along Novaya Zemlya to the north; along Novaya Zemlya to the south into the Kara Gates Strait; from Novaya Zemlya to the Yamal Peninsula (northeast and southeast); to the shores of Novaya Zemlya from the Yamal peninsula (north-

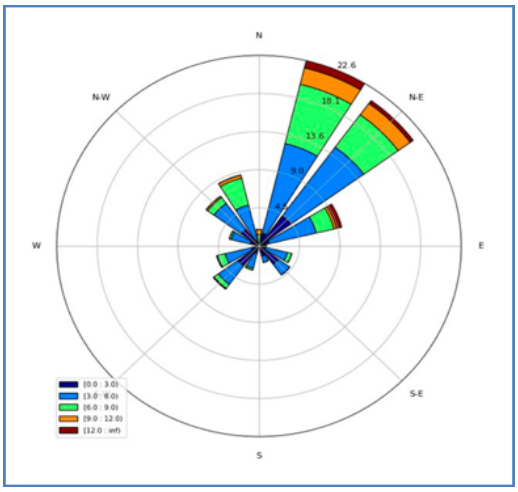


*Figure 14. Ice drift rose in the Kara Sea (2011-2015).*

west) or from the Northern Earth (south-west). Such a variety of directions is determined by the synoptic conditions over the Kara Sea and over the Arctic basin as a whole.

Frequently during the study period there was an ice drift directed along Novaya Zemlya to the north (37%), to the pole or the Barents Sea. The eastern and western directions arose in the same number of cases (24% each), the southern one - 17 %. The highest velocities were observed in the northeast and north-north-east directions (from 6 to 12 m/sec). The variability of drift in the sea was very high: in very rare cases one type of drift continued for more than two decades.

Eastern drift, directed from the shores of No-vaya Zemlya, was most frequent in March and in May. Its speed was small, 3-4 m/sec. The only case of high speed connected with this type of drift was observed in the second decade of March 2011 (up to 12 m/s) when an extensive cyclone developed in the north of Novaya Zemlya.

The ice drift directed to the south-south-west toward the Kara Gates Strait was most likely in May-June, when the speed was not more than 5 m/sec. Its appearance in winter was characterized by higher speeds, especially in the water area between Cape Zhelaniya and Taimyr Peninsula (in the third decade of February 2013 velocities reached 10 m/s).

***Okhotsk Sea.*** Sea ice in this area has the re-gional origin. The ice cover starts to develop in November in the north-western part of the sea. The emerged ice drifts along the shore in the south-eastern direction, and the ice development process in the north-western part of the sea continues. The maximum sea ice cover is observed in February-March. It can extend over the whole area of the sea, leaving only the near-shore region off the Kamchatka peninsula, the most remote part from the continent, however in some years it can be substantially smaller, covering less than 40% of the whole sea area. Changes from year to year are quite high: the standard deviation is 182000 km$^2$, being 22% of the average February-March sea ice area (834000 km$^2$). The tendency of decrease of the winter sea ice area is described by 6.6% loss of the ice per decade.

The process of melting ice cover in the Okhotsk Sea starts in the second half of March, becomes stronger in April and May; sea becomes ice-free during June. During summer the sea is also ice-free. The average sea ice area in June amounts to 19800 km$^2$ with the standard deviation of 18400 km$^2$, which is 92.8% from the average. That high variability prevents a statistically significant conclusion about the trend.

Ice formation in the Okhotsk Sea begins in November in the north-western part of the sea. The maximum area of the ice cover is observed in February-March.

In the last 5 years ice formation in the Okhotsk Sea began in the third decade of October - the second decade of November in shallow coastal areas. Further, the nilas and young ice began to form in the open water in the north-western part of the sea (island of Iona). In the more southerly regions (southeast coast of Sakhalin, Terpenia Bay), the first signs of ice freezing were observed in the first half of December. In the fall 2016, ice formation was noted 1-2 decades earlier compare to previous years.

In recent years there have been negative anomalies of the area occupied by sea ice. In the Shelikhov Bay, mainly young winter ice (up to 30 cm) predominated throughout the winter with the inclusion of individual zones of a one-year thin ice (30-70 cm). Due to the remote drift, the ice here is constantly updated and doesn't have time to reach a greater thickness. The zone of accumulation of ice was noted only in the Yamsk Bay, due to the compression and layering of ice; it reached thickness of 70-120 cm.

The maximum development of ice cover was, as a rule, in the end of March. From 2013 to 2016 the maximum ice cover was observed in the first half of March, in 2017 – in early February. Fig. 15 shows the position of the edge of drifting ice at the time of maximum ice cover over the past five years.

In the northern and north-western parts of the sea, along the coast, the polynya covered by nilas, was preserved throughout the entire season. Along the eastern coast of Sakhalin there is also a quasi-stationary polynya formed during the squeezing north-westerly wind, behind which there was always a strip of annual ice (thin with medium inclusion) brought here from the north-western part of the sea. East of this strip observed was a vast zone of young ice with the inclusion of annual thin ice of the local origin, brought here from more northern areas.

The first signs of the ice cover destruction were noted in the southern part of the sea (near the island of Hokkaido, the Strait of La Perouse) in the second half of March – early April, which corresponds to climatic data. To the east of Sakhalin, ice began to melt at the end of March and beginning of April, and completely thawed in the first half of June.

Sakhalin Bay and the area to the north of it became ice-free in the second half of June, although in 2012/13 ice stayed there until the end of July. The longest ice remained in the Shantar Sea.

Fast ice in the Okhotsk Sea was formed only in the shallow bays and inlets, as well as in the Amur estuary. During the first three weeks after beginning of ice formation, fast ice covered the bays of Sakhalin Island (Baikal, Severny, Odoptu, Piltun, Chayvo, Nyisky, Nabilsky), where its destruction also occurred in the second half of May. The thickness of fast ice in the northern part of Sakhalin reached 160 cm or more.

The steady north-westerly wind and constant currents determined the general direction of ice drift to the south-southeast practically on the whole water area, with the exception of the Shelikhov Bay and the exit from it, where there was a remote south-west drift. The southern component in the direction of the wind appeared more often from the beginning of April. The average drift velocities were 5-15 miles/day for the eastern part of the sea and 3-10 miles/day for the western part.

In general, the ice cover variability in the Okhotsk Sea has been highly mutable in the recent years.

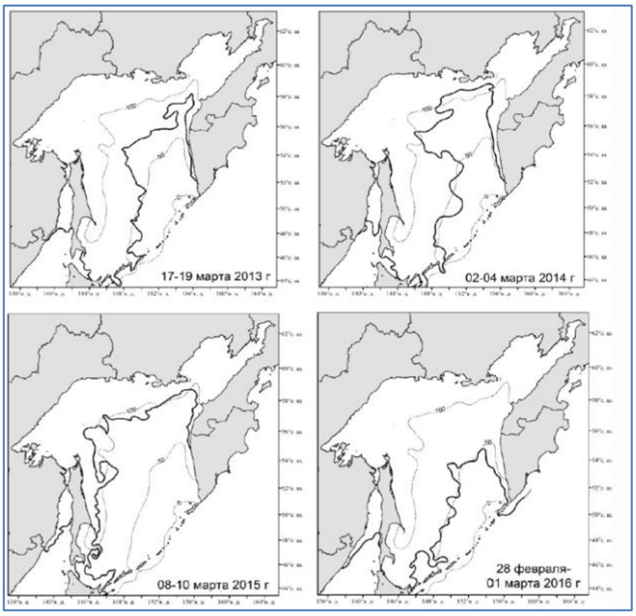


***Figure 15.*** *Position of the edge of the drifting sea ice in the Okhotsk Sea during the period of maximum ice area.*

*Relevant publication:* *Volkov, V., Demchev, D., & Ivanov, N. (2017). Validation of the Model Obtained Ice Drift Fields Based on Satellite Derived Data Using a Vector Correlation Indexes in an Invariant Form. Journal of Shipping and Ocean Engineering, 6, 250-261.*

*Demchev, D., Volkov, V., Kazakov, E., & Sandven, S. (2017). Feature tracking for sea ice drift retrieval from SAR images. IEEE International Geoscience and Remote Sensing Symposium (IGARSS). doi:10.1109/igarss.2017.8126963.*

*Demchev, D., Volkov, V., Kazakov, E., Alcantarilla, P. F., Sandven, S., & Khmeleva, V. (2017). Sea Ice Drift Tracking from Sequential SAR Images Using Accelerated-KAZE Features. IEEE Transactions on Geoscience and Remote Sensing, 55(9), 5174-5184.*

# ANNEX: Programme of the Nansen Centre's 25th Anniversary Symposium

**12 October, Thursday** Petrovsky Hall, St. Petersburg State University

| | |
|---|---|
| 09:30-10:00 | Opening. *Prof. Nikolay Filatov, President, Nansen Centre, Petrozavodsk, Russia*<br>Welcome speeches:<br>*Mr. Dag Malmer Halvorsen, Consul General of Norway in St. Petersburg*<br>*Prof. Sergey Aplonov, Vice-Rector, St. Petersburg State University, St. Petersburg, Russia* |
| 10:00-10:30 | St. Petersburg Nansen Centre: 25 years of environmental and climate research<br>*Dr. Leonid Bobylev, Director, Nansen Centre, St. Petersburg, Russia* |
| 10:30-10:55 | From Waves and Ocean Remote Sensing to Climate and Climate Policy - 25 years of fruitful collaboration with NIERSC<br>*Prof. Klaus Hasselmann and Prof. Hartmut Grassl, Max-Planck Institute for Meteorology, Hamburg, Germany* |
| 10:55-11:20 | Studies of the atmosphere, hydrosphere and educational programs of St. Petersburg State University<br>*Prof. Kirill Chistyakov, Director, Earth Sciences Institute, St. Petersburg State University/ Vice-President, Russian Geographic Society, St. Petersburg, Russia* |
| 11:40-12:05 | Arctic sea ice and processes in the Marginal Ice Zone: a brief review<br>*Prof. Ola M. Johannessen, President, Nansen Scientific Society, Bergen, Norway* |
| 12:05-12:30 | Arctic in the context of Paris Agreement<br>*Prof. Vladimir Kattsov, Director, Voeikov Main Geophysical Observatory, St. Petersburg, Russia* |
| 14:00-14:25 | Climate Change and Melting Glaciers and Ice Sheets - From Arctic to High Andes<br>*Dr. Sebastian Mernild, Director, Nansen Centre, Bergen, Norway* |
| 14:25-14:50 | Research activities of the Arctic and Antarctic Research Institute in the Arctic<br>*Prof. Alexander Makarov, Director, Arctic and Antarctic Research Institute, St. Petersburg, Russia* |
| 14:50-15:15 | Monitoring and modelling atmospheric gases<br>*Prof. Yury Timofeev and Prof. Sergey Smyshlyaev, St. Petersburg State University, St. Petersburg, Russia* |
| 15:15-15:40 | Calcifying phytoplankton role in $CO_2$ dynamics in the atmosphere-ocean system at subpolar and polar latitudes<br>*Prof. Dmitry Pozdnyakov, Nansen Centre, St. Petersburg, Russia* |
| 15:40-16:05 | Largest lakes of Eurasia: integrated studies of ecosystems<br>*Prof. Nikolay Filatov, Corresponding Member RAS, President, Nansen Centre/ Councillor RAS, Northern Water Problems Institute, Petrozavodsk, Russia* |
| 16:25-16:50 | Ice climatology of polar lakes<br>*Prof. Matti Leppäranta, University of Helsinki, Helsinki, Finland* |
| 16:50-17:15 | Integrated Arctic observation system (INTAROS)<br>*Prof. Stein Sandven, Nansen Centre, Bergen, Norway* |
| 17:15-17:40 | The impact of climate change on wind energy in Europe<br>*Dr. Richard Davy, Nansen Centre, Bergen, Norway* |

**13 October, Friday** Nansen Centre

| | |
|---|---|
| 10:00-10:25 | Global warming in the Arctic: role of atmospheric transport and solar radiation<br>*Prof. Genrikh Alekseev, Arctic and Antarctic Research Institute, St. Petersburg, Russia* |
| 10:25-10:40 | Seasonal and interannual variability of heat fluxes in the Barents Sea region<br>*Dr. Igor Bashmachnikov, St. Petersburg State University/Nansen Centre, St. Petersburg, Russia* |
| 10:40-10:55 | Atmospheric heat advection in the Kara Sea region<br>*Dr. Alla Yurova, St. Petersburg State University/Nansen Centre, St. Petersburg, Russia* |
| 11:20-11:45 | Arctic climate change: anomalies and trends<br>*Prof. Igor Mokhov, Academician RAS, Director, Obukhov Institute of Atmospheric Physics, Moscow, Russia* |
| 11:45-12:10 | Effects of changing Arctic on mid-latitude weather and climate<br>*Prof. Timo Vihma, Finnish Meteorological Institute, Helsinki, Finland* |
| 12:10-12:35 | Arctic warming and cold weather over continents - great scientific challenge<br>*Prof. Valentin Meleshko, Voeikov Main Geophysical Observatory, St. Petersburg, Russia* |
| 12:35-12:50 | Effects of surface temperature anomalies in the Arctic on 2-m air temperature in Europe and Northern Asia<br>*Dr. Natalia Gnatiuk, Nansen Centre, St. Petersburg, Russia* |
| 14:00-14:15 | A new methodology of remote sensing determination of $CO_2$ partial pressure dynamics in surface ocean due to E. huxleyi blooms<br>*Dmitry Kondrik, Nansen Centre/Arctic and Antarctic Research Institute, St. Petersburg, Russia* |
| 14:15-14:35 | Applied meteorological and oceanographic research at NIERSC<br>*Dr. Vladimir Volkov, Nansen Centre, St. Petersburg, Russia* |
| 14:35-14:50 | Operational algorithm for automated sea-ice retrieval in the Arctic using SAR data<br>*Dr. Natalia Zakhvatkina, Arctic and Antarctic Research Institute/Nansen Centre, St. Petersburg, Russia* |
| 14:50-15:05 | Sea ice drift retrieval from satellites<br>*Denis Demchev, Arctic and Antarctic Research Institute/Nansen Centre, St. Petersburg, Russia* |
| 15:05-15:20 | NIERSC data archiving and processing system for research and environmental monitoring in the Arctic<br>*Eduard Kazakov, Nansen Centre, St. Petersburg, Russia* |
| 15:45-16:00 | Introducing Climate Service Centre Germany: think tank for climate services<br>*Dr. Lola Kotova, Climate Service Centre Germany (GERICS), Hamburg, Germany* |
| 16:00-16:15 | Presentation of the Nansen-Zhu Centre (NZC)<br>*Prof. Jianqi Sun, Nansen-Zhu Centre, Beijing, China* |
| 16:15-16:30 | Presentation of the Nansen Environmental Research Centre, India (NERCI)<br>*Dr. Ajith Joseph, Nansen Environmental Research Centre, Kochi, Kerala, India* |

# PUBLICATIONS

## Book

*Pozdnyakov, D.,* *Pettersson, L., and Korosov, A.* (2017). *Exploring the marine ecology from space: Experience from Russian-Norwegian cooperation.* Springer, 215 pp.

## Refereed Papers

*Davy, R., N. Gnatiuk, L. Pettersson, L. Bobylev* (2017). Climate change impacts on wind energy potential in the European domain with a focus on the Black Sea. *Renewable and Sustainable Energy Reviews*, 81, 1652-1659

*Bashmachnikov, I., M.A. Sokolovskiy, T.V. Belonenko, D.L. Volkov, P.E. Isachsen and X. Carton* (2017). On the vertical structure and stability of the Lofoten vortex in the Norwegian Sea. *Deep-Sea Research I*, 128, 1-27

*Ciani, D., X. Carton, A.C. Barbosa Aguiar, Á. Peliz, I. Bashmachnikov, F. Ienna, B. Chapron, R. Santoleri*. (2017). Surface signature of Mediterranean water eddies in a long-term high-resolution simulation. *Deep-Sea Research I*, 130, 12-29, https://doi.org/10.1016/j.dsr.2017.10.001.

*Belonenko, T.V., Bashmachnikov, I.L., Koldunov, A.V., Kuibin, P.A,* (2017). On the Vertical Velocity Component in the Mesoscale Lofoten Vortex of the Norwegian Sea. *Izvestiya RAS, Atmospheric and Oceanic Physics*, 53 (6), 641-648

*Kraev, G., Schulze, E.D., Yurova, A., Kholodov, A., Chuvilin, E., & Rivkina, E.* (2017). Cryogenic Displacement and Accumulation of Biogenic Methane in Frozen Soils. *Atmosphere*, 8(6), 105.

*Selyuzhenok, V., Mahoney, A.R., Krumpen, T., Castellani, G., Gerdes, R.* (2017). Mechanisms of fast ice development in the southeastern Laptev Sea: A Case study for winter of 2007/08 and 2009/10. *Polar Research*, 36, doi: 10.1080/17518369.2017.1411140.

*Kovalevsky, D.V., Hewitt, R., de Boer, C., Hasselmann, K.* (2017). A dynamic systems approach to the representation of policy implementation processes in a multi-actor world. *Discontinuity, Nonlinearity, and Complexity,* 6(3), 219-245. DOI: 10.5890/DNC.2017.09.001

*Kondrik, D., Pozdnyakov, D., Pettersson L.* (2017). Multi-year tendencies in *E. huxleyi* blooms over latitudinally and meridianally distanced marine environments in the northern hemisphere as revealed from satellite observations during 1998-2013. *Earth Observation from Space*, 2, 1-12 *(in Russian*).

*Kondrik, D., Pozdnyakov, D., Pettersson, L.* (2017). Particulate inorganic carbon production within *E. huxleyi* blooms in subpolar and polar seas: A satellite time series study (1998-2013). *International Journal of Remote Sensing,* 38:22, 6179-6205, doi: 10.1080/01431161.2017.1350304.

*Korosov, A., Pozdnyakov, D., Shuchman, R., Sayers, Sawtell, Moiseev, A.* (2017). Bio-optical retrieval algorithm for the optically shallow waters of Lake Michigan. I. Model description and sensitivity/robustness assessment. *Limnologia*. 3, 79-93.

*Zakhvatkina, N.Yu., A. Korosov, S. Muckenhuber, S. Sandven, and M. Babiker* (2017). Operational algorithm for ice–water classification on dual-polarized RADARSAT-2 images. *The Cryosphere*, 11, 33-46, doi:10.5194/tc-11-33-2017.

*Demchev, D., V. Volkov, E. Kazakov, P.F. Alcantarilla, S. Sandven, and V. Khmeleva* (2017). Sea Ice Drift Tracking from Sequential SAR Images Using Accelerated-KAZE Features. *IEEE Transactions on geoscience and Remote Sensing*, 55(9), 5174-5184, (http://ieeexplore.ieee.org/document/7938663/).

*Vesman, A., B. Ivanov, V. Volkov* (2017). Changes in thermohaline system on the west Spitsbergen shelf since 1950 to present time. *Czech Polar Reports*, 7 (1), 62-73.

## Other Papers

*Bashmachnikov, I., Belonenko, T.V., Kuibin, P.A.* (2017). Application of the theory of columnar Q-vortices with helical structure to derivation of dynamic properties of the Lofoten Vortex in the Norwegian Sea. *Vestnik SPbSU (Bulletin of St. Petersburg University), Earth Sciences*, 62 (3), 221-236, doi: 0.21638/11701/spbu07.2017.301.

*Krakovska, S.V., Palamarchuk, L.V., Gnatiuk, N.V., Shpytal, T.M., Shedemenko, I.P.* (2017). Changes in precipitation distribution in Ukraine for the 21st century based on data of regional climate model ensemble. *Geoinformatika,* 4(64), 62-74.

*Shalina, E., Bobylev, L*. (2017). Sea ice transformations in the Arctic from satellite observations. *Current problems in remote sensing of the Earth from space*, 14(6), 28-41, doi: 10.21046/2070-7401-2017-14-6-28-41 (in Russian).

*Bobylev, L.P., Romanyuk, L.P., Pozdnyakov, D.V.* (2017). Experience of International Cooperation in the Research Area of Climate Change in high Northern Latitudes. *Prikladnaya Ecologia (Applied Ecology),* 3(49), 82-86 *(in Russian).*

*Zakhvatkina N., S. Mikhaltseva* (2017). Identification of the multiyear floes. Section 3.4 in: Smirnov V.G., ed. *Detection of the dangerous ice features near engineering objects of economic activity in the shelf areas of the Arctic seas using remote sensing data*. Methodical manual. St. Petersburg, AARI, 63-71 (*in Russian*).

*Volkov, V.A., Demchev, D.M. and Ivanov, N.E.* (2017). Validation of the model obtained ice drift fields based on satellite derived data using a vector correlation indexes in an invariant form. *Journal of Shipping and Ocean Engineering (JSOE)*, 7(6), 250-261.

## Conference Proceedings

*Alekseev G., S. Kuzmina, A. Urazgildeeva, and L. Bobylev*. Influence of atmospheric energy transport on amplification of winter warming in the Arctic. Poster. *International Conference on Arctic Science: Bringing Knowledge to Action,* Reston, Virginia, USA, April 24-27, 2017

*Alekseev G., S. Kuzmina, and N. Glok.* Influence of SST anomalies in low latitudes on atmospheric heat transport to the Arctic. Poster. *EGU General Assembly 2017,* Viena, Austria, 23-28 April 2017

*Bashmachnikov, I.L.* Seasonal and interannual variations in the dynamic and thermal fronts of the Barents, Norwegian and Greenland Seas. Proceedings of the conference *"Russian seas: science, security and resources"*, pp. 29-30, Sebastopol, Russia, 3-7 October 2017

*Bashmachnikov, I.L., A.Yu. Yurova, L.P. Bobylev, A.V. Vesman*. On links between variations of oceanic and atmospheric heat fluxes to the Barents Sea region. Proceedings of the conference *"Russian seas: science, security and resources"*, pp. 29-30, Sevastopol, Russia, 3-7 October 2017

*Gnatiuk, N., Vihma, T., Bobylev, L.* Effects of surface temperature anomalies in the Northern Hemisphere on 2-m air temperature in Europe and Northern Asia. *Arctic Science Summit Week (ASSW 2017),* Prague, Czech Republic, 4-7 April 2017

*Vihma, T., Gnatiu,k N., Bobylev, L.* Effects of Earth surface temperature anomalies on 2-m air temperature in the Northern Hemisphere. *US CLIVAR Workshop,* Washington, DC, USA, 1-3 February 2017

*Krakovska, S., Chyhareva, A., Cheva,l S., Gnatiuk, N.* Shifts of season duration in the Pannonia region in the period 1961-2010. *3rd PannEx Workshop*, Cluj-Napoca, Romania, 20-22 March 2017

*Krakovska, S., Palamarchuk, L., Chyhareva, A., Gnatiuk, N., Shpytal, T.* Some hydrothermal characteristics of the Pannonian region under the current climate change. *3rd PannEx Workshop*, Cluj-Napoca, Romania, 20-22 March 2017

*Gnatiuk, N., Vihma, T., Bobylev, L.* Lagged effects of Earth surface temperature anomalies on northeast European weather. *3rd PEEX Science Conference*, Moscow, Russia, 19-22 September 2017.

*Shalina, E., Bobylev, L*. Sea ice transformations in the Arctic from satellite observations. *Abstracts of 15th Conference "Current problems in remote sensing of the Earth*

*from space"*, Moscow, 13-17 November 2017. http://smiswww.iki.rssi.ru/d33_conf/thesisshow.aspx?page=144&thesis=6169 (in Russian).

*Shalina, E., Bobylev, L.* Sea ice transformations in the Arctic from the period of satellite observations. *Proceedings of the conference "Hydrometeorology and Ecology: Scientific and Educational Achievements and Prospects for the Development"*, St. Petersburg, 19–20 December 2017, 484-486 (in Russian).

*Hewitt, R., Kovalevsky, D.V., de Boer, C., Hasselmann, K.* (2017). Modelling actors' influence on land use change: a dynamic systems approach. In: Bregt, A., Sarjakoski, T., Lammeren, R. van, Rip, F. (Eds.). Societal Geo-Innovation: short papers, posters and poster abstracts of the 20th AGILE Conference on Geographic Information Science. Wageningen University, 9-12 May 2017, Wageningen, the Netherlands. ISBN 978-90-816960-7-4. Accessible through https://agile-online.org/index.php/conference/proceedings/proceedings-2017.

*Zaitsev L.V., Kovalevsky D.V.* (2017). Strategies of price formation and inventory management under stochastic demand caused by 'herding behaviour' of consumers. *The Third Readings in Memory of Prof. B.L. Ovsievich "Economic-Mathematical Studies: Mathematical Models and Information Technologies" – Proceedings of the All-Russian Conference*, 7-9 November 2017, St. Petersburg, Russia, 104-107 *(in Russian).*

*Pozdnyako,v D., Kondrik, D., Pettersson L.* Inorganic carbon production by coccolithophores: a space borne study. *The 3rd Pan-Eurasian Experiment (PEEX) Science Conference*, 19-22 September 2017, Moscow, Russia

*Kondrik, D., Pozdnyakov, D., Pettersson, L.* A spaceborne study on *E. huxleyi* bloom extent dynamics at high northern latitudes. Poster. *The 3rd Pan-Eurasian Experiment (PEEX) Science Conference*, 19-22 September 2017, Moscow, Russia

*Bobylev, L., Volkov, V., Kazakov, E., Demchev, D.* Satellite data based automated arctic sea ice monitoring system. *Proceedings of the Eight EuroGOOS International Conference: Operational Oceanography Serving Sustainable Marine Development,* 3-5 October 2017, Bergen, Norway, 409-414.

*Volkov, V.A., Kazakov, E.E., Demchev, D.M., Zakhvatkina, N.Y., & Khmeleva, V.S.* A Monitoring System of Ice Conditions to Support Geological Surveying in Arctic Seas. Abstracts of the International Conference *Geomodel 2017*, available at http://www.earthdoc.org/publication/publicationdetails/?publication=43784

*Mushta, A.V., Volkov, V.A., Demchev, D.M.* Investigation of large-scale structures of ice drift in the Arctic Basin based on satellite remote sensing data. *Symposium on Atmospheric Radiation and Dynamics "ISARD-2017"*, 27-30 June 2017, St. Petersburg-Petrodvorets.

*Demchev, D., Volkov, V., Kazakov, E.,* Sandven, S. Feature Tracking for sea ice drift retrieval from SAR images. *Proceedings of the Geoscience and Remote Sensing Symposium (IGARSS)*, 2017, 330-333.

*Khmeleva, V.S., Volkov, V.A, Demchev, D.M.* Methods of automated calculation of sea-ice drift fields from sequential radar images of the Sentinel satellite system. *XXX All-Russian Symposium "Radar Survey of Natural Environments"*, 18-19April 2017, A.F. Mozhaisky Academy, St. Petersburg

*Mushta, A.V., V.A. Volkov, D.M. Demchev.* On the climatic changes in the large-scale field of ice and ice drift in the Arctic Ocean at the turn of the 20th and 21st centuries. *II All-Russian Conference of Young Scientists "Integrated Studies of the World Ocean"*, 10-15April 2017, Institute of Oceanography RAS, Moscow

*Kazakov, E., Volkov, V., Demchev, D.* Arctic sea ice monitoring system based on public domain satellite radar data. In proceedings of *2nd International Conference on Applied Science «Geodesy, Cartography, Geoinformatics and Cadastre. From idea to application»*, 8-10November 2017, St. Petersburg, Russia, 33-39

*Shirshova, V., Kazakov, E.* Automated monitoring system of ice regime of major rivers in the northern latitudes based on open satellite data. In proceedings of *2nd International Conference on Applied Science «Geodesy, Cartography, Geoinformatics and Cadastre. From idea to application»*, 8-10 November 2017, St. Petersburg, Russia, 86-92

*Shabalina, E., Kazakov, E.* Combined algorithm for automated classification of radar images with C-SAR (Sentinel-1 A/B) sensor data. In proceedings of *2nd International Conference on Applied Science «Geodesy, Cartography, Geoinformatics and Cadastre. From idea to application»*, 8-10 November 2017, St. Petersburg, Russia, 80-85

*Andreeva, T., Sukhacheva, E., Aparin, B., Lazareva, M., Kazakov, E.* Medium-scale digital soil mapping as a basis for regional policy on environmental management on the example of Leningrad Region. In proceedings of *2nd International Conference on Applied Science «Geodesy, Cartography, Geoinformatics and Cadastre. From idea to application»*, 8-10 November 2017, St. Petersburg, Russia, 262-266

*Shabalina, E., Kazakov, E.* Combined method of automated urban mapping with Sentinel-1A/B data based on textural and noise radar images characteristics. In proceedings of *International conference for young scientists «Theory and practice of modern geographical research»*, 7-9 April 2017, St. Petersburg, Russia, 583-587

*Vesman, A.V., Ivanov, B.V., Volkov, V.A.* Changes in the ice cover in the northern regions of the Barents Sea from 1997 to 2016. Conference *"Russian Seas: Science, Security, Resources"*, 3-7 October 2017, Sevastopol, Russia

*Vesman, A.V., Bashmachnikov, I.L., Ivanov, B.V.* The links between variations of oceanic heat flux trough the Fram strait and the sea ice conditions to the north of Svalbard Archipelago. *Svalbard Science Conference*, 6-8 November 2017, Oslo, Norway

*Demchev, D., Volkov, V., Kazakov, E., & Sandven, S.* Feature tracking for sea ice drift retrieval from SAR images. 2017 IEEE International Geoscience and Remote Sensing Symposium (IGARSS), 23-28 July, Texas, USA. doi:10.1109/igarss.2017.8126963.

# The Nansen Centre in St. Petersburg is the member of the international research network

**NANSEN ENVIRONMENTAL AND REMOTE SENSING CENTER**

Thormøhlens gate 47
N-5006 Bergen
NORWAY
Phone: +47 55205800
Fax: +47 55205801
e-mail: admin@nersc.no

Svalbard research park
N-9171 Longyearbyen,
Svalbard
Phone: +47 79026447
http://www.nersc.no

Mohn-Sverdrup Center
Global Ocean Studies - Operational Oceanography

GC RIEBER
Climate Research Institute

**NANSEN INTERNATIONAL ENVIRONMENTAL AND REMOTE SENSING CENTRE**

14th. Line V.O. 7A, office 34-35
199034 Saint Petersburg, RUSSIA
Phone: +7 812 324 5103/01
Fax: +7 812 324 5102
E-mail: adm@niersc.spb.ru
http://www.niersc.spb.ru

**NANSEN ENVIRONMENTAL RESEARCH CENTRE - INDIA**

6A, Oxford Business Centre, Sreekandath Road
Kochi 682016 Kerala - INDIA
Phone: +91 484 2383351
Fax: +91 484 2353124
E-mail: nerci@ipath.net.in
http://www.nerci.in

**NANSEN-ZHU INTERNATIONAL RESEARCH CENTRE**

c/o Institute of Atmospheric Physics,
Chinese Academy of Sciences,
PO Box 9804, Beijing 100029, CHINA
Phone: +86-10-62063256
E-mail: nzc@mail.iap.ac.cn
http://nzc.iap.ac.cn

NANSEN-TUTU CENTRE
MARINE ENVIRONMENTAL RESEARCH

**NANSEN-TUTU CENTRE FOR MARINE ENVIRONMENTAL RESEARCH**

c/o Marine Research Institute
University of Cape Town
Rodebosh 7701 - SOUTH AFRICA
Phone: + 27 21 650 3281
E-mail: bjorn.backeberg@uct.ac.za
http://ma-re.uct.ac.za/nansen-tutu-centre/

**NANSEN INTERNATIONAL CENTRE FOR COASTAL, OCEAN AND CLIMATE STUDIES**

c/o Bangladesh Centre for Advanced Studies
(BCAS)
House 10, Road 16A
Gulshan-1, Dhaka- 1212, BANGLADESH
Phone: +8801730019213
E-mail: atiq.rahman@bcas.net

**TERRA ORBIT AS**

Thormøhlensgate 47
N-5006 Bergen, NORWAY
Phone: +47 55205800
Fax: +47 55205801
e-mail: terraorbit@terraorbit.com
http://www.terraorbit.com

Nansen Scientific Society

**NANSEN SCIENTIFIC SOCIETY**

c/o NERSC,
Thormøhlensgate 47
N-5006 Bergen, NORWAY
Phone: +47 55205800
Fax: +47 55205801
e-mail: ola.johannessen@nersc.no

## Address/Links


**Scientific Foundation "Nansen International Environmental and Remote Sensing Centre"**

14th Line 7, Vasilievsky Island
199034 St. Petersburg, RUSSIA

Phone: +7 (812) 324 51 01
Fax: +7 (812) 324 51 02

E-mail: adm@niersc.spb.ru
http://www.niersc.spb.ru